The effect of inter-granular constraints on the response of polycrystalline piezoelectric ceramics at the surface and in the bulk

Hossain, Mohammad J.; Wang, Zhiyang; Khansur, Neamul H.; Kimpton, Justin A.; Oddershede, Jette; Daniels, John E.

Published in:
Applied Physics Letters

Link to article, DOI:
10.1063/1.4962125

Publication date:
2016

Document Version
Publisher's PDF, also known as Version of record

AIP | Applied Physics Letters

The effect of inter-granular constraints on the response of polycrystalline piezoelectric ceramics at the surface and in the bulk

Mohammad J. Hossain, Zhiyang Wang, Neamul H. Khansur, Justin A. Kimpton, Jette Oddershede, and John E. Daniels

Citation: Applied Physics Letters **109**, 092905 (2016); doi: 10.1063/1.4962125
View online: http://dx.doi.org/10.1063/1.4962125
View Table of Contents: http://scitation.aip.org/content/aip/journal/apl/109/9?ver=pdfcov
Published by the AIP Publishing

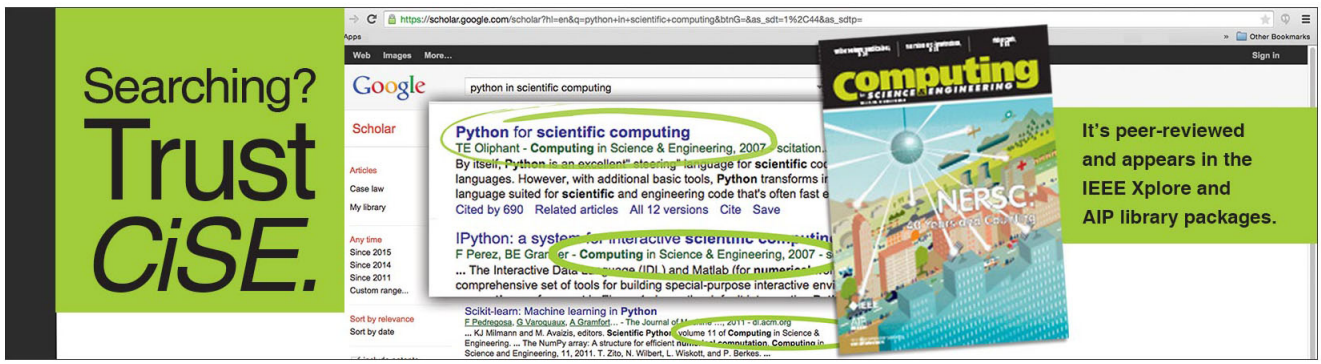

The effect of inter-granular constraints on the response of polycrystalline piezoelectric ceramics at the surface and in the bulk

Mohammad J. Hossain,[1] Zhiyang Wang,[1,2] Neamul H. Khansur,[1,3] Justin A. Kimpton,[2] Jette Oddershede,[4] and John E. Daniels[1,a)]
[1]*School of Materials Science and Engineering, UNSW Australia, Sydney, New South Wales 2052, Australia*
[2]*Australian Synchrotron, 800 Blackburn Road, Clayton, Victoria 3168, Australia*
[3]*Department of Materials Science, University of Erlangen-Nürnberg, Erlangen 91058, Germany*
[4]*NEXMAP, DTU Physics, Fysikvej, 2800 Kongens Lyngby, Denmark*

(Received 24 May 2016; accepted 20 August 2016; published online 31 August 2016)

The electro-mechanical coupling mechanisms in polycrystalline ferroelectric materials, including a soft $PbZr_xTi_{1-x}O_3$ (PZT) and lead-free $0.9375(Bi_{1/2}Na_{1/2})TiO_3$-$0.0625BaTiO_3$ (BNT-6.25BT), have been studied using a surface sensitive low-energy (12.4 keV) and bulk sensitive high-energy (73 keV) synchrotron X-ray diffraction with *in situ* electric fields. The results show that for tetragonal PZT at a maximum electric field of 2.8 kV/mm, the electric-field-induced lattice strain (ε_{111}) is 20% higher at the surface than in the bulk, and non-180° ferroelectric domain texture (as indicated by the intensity ratio I_{002}/I_{200}) is 16% higher at the surface. In the case of BNT-6.25BT, which is pseudo-cubic up to fields of 2 kV/mm, lattice strains, ε_{111} and ε_{200}, are 15% and 20% higher at the surface, while in the mixed tetragonal and rhombohedral phases at 5 kV/mm, the domain texture indicated by the intensity ratio, $I_{111}/I_{11\bar{1}}$ and I_{002}/I_{200}, are 12% and 10% higher at the surface than in the bulk, respectively. The observed difference in the strain contributions between the surface and bulk is suggested to result from the fact that surface grains are not constrained in three dimensions, and consequently, domain reorientation and lattice expansion in surface grains are promoted. It is suggested that the magnitude of property difference between the surface and bulk is higher for the PZT than for BNT-6.25BT due to the level of anisotropy in the strain mechanism. The comparison of the results from different methods demonstrates that the intergranular constraints have a significant influence on the electric-field-induced electro-mechanical responses in polycrystalline ferroelectrics. These results have implications for the design of higher performance polycrystalline piezoelectrics. *Published by AIP Publishing.* [http://dx.doi.org/10.1063/1.4962125]

Piezoelectric ceramic materials play an important role as sensors and actuators for the design of smart devices. For many years, lead zirconate titanate (PZT) has been the material of choice for the electro-mechanical components. Due to the international consent towards removing toxic substances from the electronic and electrical equipment and the harmful effects of Pb from the environment,[1] it is necessary to find lead-free piezoelectric materials with comparable properties to those of PZT. Promising lead-free piezoelectrics are mainly based on solid solutions incorporating either $Bi_{1/2}Na_{1/2}TiO_3$ (BNT) or $Na_xK_{1-x}NbO_3$ (KNN).[2–7] Although lead-free compositions of piezoelectric materials have been reported with excellent properties, no single composition has been identified with the potential for the replacement of PZT over the range of technological application conditions. To further improve the electro-mechanical properties of these materials, a comprehensive understanding of the underlying microscopic origin of the electric-field-induced strain is requisite.

The electric-field-induced macroscopic strain in piezoelectric materials has been shown to originate from at least three structural contributions: (i) intrinsic piezoelectric lattice strain resulting from the distortion of the unit cell, (ii) electric-field-induced non-180° (Refs. 8 and 9) and 180° (Ref. 10) domain wall motion, and (iii) electric-field-induced phase transformations.[11–13] The above mentioned structural contributions to the macroscopic strain in the polycrystalline piezoelectric materials under a mechanical stress or electrical field are more complex than in single crystals due to the coupling of strain between neighboring grains or within the clusters of grains. The exact mechanisms, which couple these strains between individual grains within the polycrystalline state, are still unknown. An example of the complexity can be found when considering a lattice strain of a given grain. Such a strain arises from both the intrinsic piezoelectric effect of that grain in its electric field environment and the compliance of the grain with other strain mechanisms in adjacent grains.[11,14] The magnitude of this compliance or intergranular coupling effect, as well as its influence on the macroscopic strain properties, is not thoroughly understood. It has also been demonstrated that the magnitude of the electric-field-induced strain response in phase change piezoelectric ceramics is highly heterogeneous at the grain scale,[15] adding further evidence to the importance of understanding the coupling of properties between grains. These local compliance effects are expected to vary the response of the polycrystalline microstructure under different constraint conditions. Most notably, at the surface of the material where the three-dimensional constrains of a bulk material become

a)Author to whom correspondence should be addressed. Electronic mail: j.daniels@unsw.edu.au. Tel.: +61 2 93855607.

two-dimensional as the stress perpendicular to the surface is relieved. The so called "skin effects" have been reported in single crystals;[16] however, a quantitative account of this effect in various polycrystalline materials is lacking.

X-ray diffraction (XRD) is a powerful tool to observe the underlying electro-mechanical coupling mechanisms in piezoelectric materials. The intrinsic lattice strain component can be calculated from diffraction peak position shifts, while the extrinsic strain caused by non-180° domain wall motion and/or phase transformations is quantified from diffraction peak relative intensity changes and splitting of symmetry dependent reflections during the application of an external field.

In the present study, the constraints of the polycrystalline state on the electro-mechanical response are directly probed in a soft PZT and $0.9375(Bi_{1/2}Na_{1/2})TiO_3$-$0.0625BaTiO_3$ (BNT-6.25BT) by contrasting the electric-field-induced response measured by a surface sensitive low-energy and bulk sensitive high-energy synchrotron XRD. Low-energy X-rays penetrate only a few micrometres into the material, and therefore only provide information from grains that directly intersect the surface or within a few grains deep. High-energy X-rays probe all grains within the sample, of which the surface grains comprise less than 1% in the present geometry. The results show that for both PZT and BNT-6.25BT, the lattice strains and domain texture changes under electric field are larger at the surface than in the bulk. The observed difference between the two measurements is related to the distinct inter-granular constraint conditions experienced by surface and bulk grains. Additionally, it is shown that the BNT-6.25BT material displayed less difference between the surface and bulk measurements than the PZT. This is attributed to the magnitude of anisotropy of the response occurring in each material.

Commercial PZT (PIC151, PI ceramics, Lederhose, Germany) and in-house processed BNT-6.25BT were used. Disc shaped samples of BNT-6.25BT were prepared by the solid state synthesis route. Details of the sample synthesis can be found elsewhere.[6] The samples for low-energy synchrotron measurements were 8 mm in diameter and polished to 1 mm thickness. The same batches of samples were used for high-energy XRD to allow a direct comparison between the surface and the bulk properties. Bar-shaped samples with dimensions of $1 \times 1 \times 6\,mm^3$ were prepared for high-energy XRD experiments. The samples were annealed at 400 °C for 30 min to remove any possible residual stresses induced from the sample preparation process. For surface sensitive XRD experiments, one of the parallel surfaces of the disk samples was sputtered with gold to a thickness of approximately 45 nm in order to allow penetration of the low-energy X-ray beam into the sample surface. The other side of the sample was coated with a silver paste electrode. For high-energy XRD measurements, silver paste electrodes were applied to two opposing $1 \times 6\,mm^2$ faces of the bar.

The surface sensitive low-energy and bulk sensitive high-energy XRD experiments were performed using the two different experimental setups as shown in Figure 1. The surface sensitive X-ray scattering experiments were carried out at the Powder Diffraction beamline of the Australian Synchrotron.[17] A monochromatic X-ray beam of energy

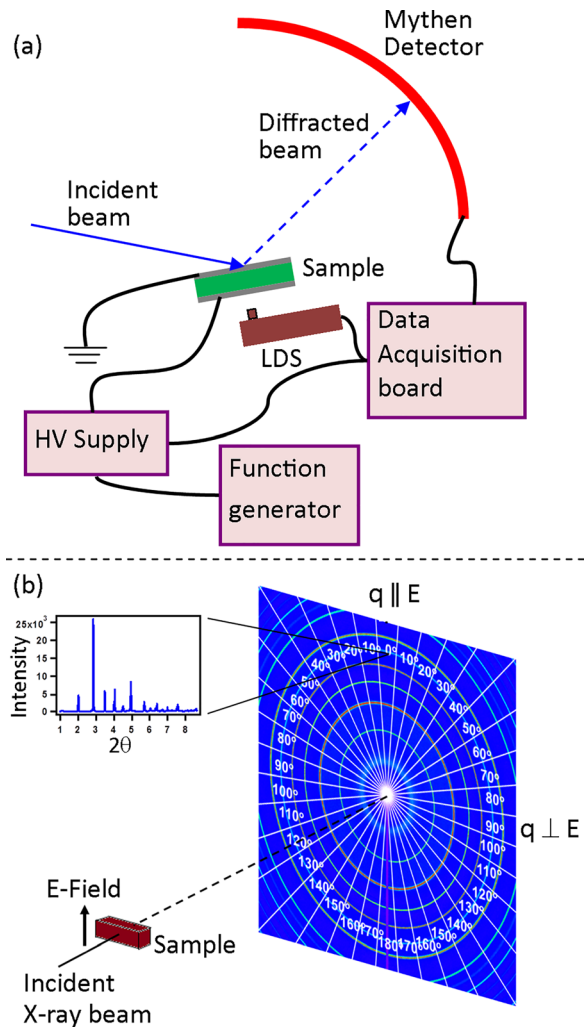

FIG. 1. Schematic diagram of the setups used for *in situ* (a) surface sensitive low-energy and (b) bulk sensitive high-energy synchrotron X-ray scattering experiments.

12.4 keV ($\lambda = 0.998$ Å) was used. XRD data were collected in reflection geometry using a Mythen detector.[18] Samples were mounted in a specially developed cell.[19] Bipolar electric fields were applied using step-triangular waveforms with a maximum amplitude of 2.8 kV/mm in 0.28 kV/mm steps for PZT and 5 kV/mm in 0.5 kV/mm steps for BNT-6.25BT. In this experimental setup (Figure 1(a)) the electric field vector was aligned approximately perpendicular to the probed 111 and 200 crystallographic lattice planes. The attenuation depth of X-rays into the surface for this geometry was calculated to be 5.4 μm for PZT and 7.8 μm for BNT-6.25BT. The approximate grain size of PZT and BNT-6.25BT was 5 μm (Ref. 20) and 1.7 μm, respectively, meaning that the probed surface layer had a thickness of approximately 1–2 grains for PZT and 4–5 grains for BNT-6.25BT. However, in both cases, the scattered intensity is dominated by grains that intersect the surface.

The bulk sensitive X-ray scattering experiments were carried out at the beamline ID15 of the European Synchrotron Radiation Facility. An X-ray beam with energy of 73 keV ($\lambda = 0.171$ Å) and dimensions $200 \times 200\,\mu m^2$ was used. The samples were placed in a specifically designed sample cell where the electric field was applied perpendicular to the incident X-ray beam direction.[21] Electric field

cycles identical to those used in the low-energy XRD experiments were applied to the samples while the diffraction images were collected in transmission geometry using a Pixium 4700 large area detector.[22] The diffraction images were radially integrated into 36 angular segments of 10° widths using the software package FIT2D.[23] In the following analysis, only the integrated data with the scattering vector parallel to the direction of the applied electric field were analyzed to make the data directly comparable with that from the surface.

The diffraction peaks were fit individually with pseudo-Voigt profile shape functions[24] to obtain diffraction peak positions, areas, and widths as a function of applied electric field. The fitted peak positions were used to calculate the lattice strain as a function of electric field. The peak intensity ratios were calculated from the fitted diffraction peak areas for symmetry dependent reflections to obtain a quantitative measure of the non-180° domain wall motion and/or any phase transformation behavior during electric field application.

A comparison between the surface sensitive low-energy and bulk sensitive high-energy XRD patterns for (111) and (200) crystallographic planes of PZT and BNT-6.25BT is shown in Figure 2. In the case of PZT (Figures 2(a) and 2(b)), the crystallographic phase is tetragonal in the initial state and remains tetragonal up to the maximum electric field amplitude of 2.8 kV/mm. At the surface, the asymmetry of the (111) peak is likely due to the coincidence of the (111) gold peak which is overlapped. For BNT-6.25BT, on the other hand, the crystallographic structure is pseudo-cubic in the initial state and mixed (rhombohedral and tetragonal) phase at 5 kV/mm. The onset of the mixed phase was found at a field strength of 2.5 kV/mm.

A comparison between the electric-field-induced lattice strain and domain texture as a function of applied electric field collected from the surface and the bulk is shown in Figure 3. In the case of the PZT sample, the electric-field-induced lattice strain and non-180° ferroelectric domain switching were observed over the full field range measured. These results are consistent with earlier results from tetragonal PZT.[25,26]

For BNT-6.25BT, the initial structure is pseudo-cubic. On the application of the electric field, only the lattice strain is observed up to a critical field strength of around 2.5 kV/mm. Here, the material transforms to a tetragonal and rhombohedral mixed phase symmetry, also consistent with the earlier results on similar compositions.[27–29] From this point, it is no longer possible to calculate lattice strains as the diffraction peaks have split due to the lower symmetry of the induced phase; however, the intensity ratios were calculated from the symmetry dependent reflections to quantify further non-180° domain wall motion in the transformed phase.

In both cases, the magnitudes of the material response, including the lattice strain and the induced domain texture changes, are consistently higher at the surface than within the bulk. In particular, for PZT, at the maximum electric field, the electric-field-induced lattice strain (ε_{111}) and non-180° domain texture as indicated by the intensity ratio

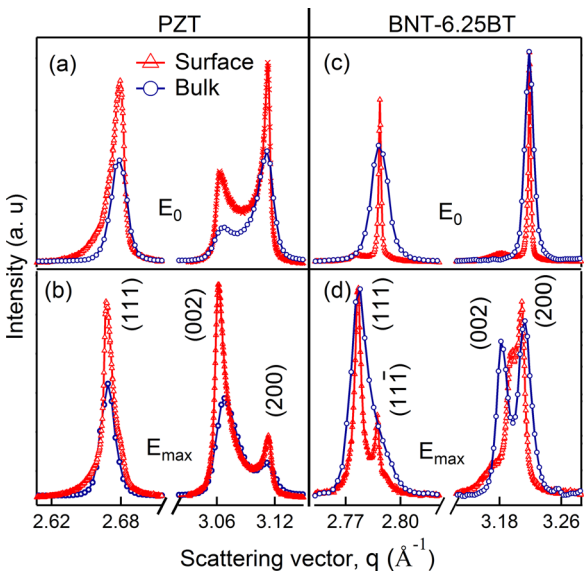

FIG. 2. Diffraction patterns near the 111 and 200 reflections of soft PZT ((a) and (b)) and BNT-6.25BT ((c) and (d)) measured using surface sensitive low-energy (red) and bulk sensitive high-energy XRD (blue) at initial zero, E_0 ((a) and (c)), and maximum electric fields, E_{max} ((b) and (d)). For direct comparison, the data are displayed as a function of the magnitude of the scattering vector q, where $q = \frac{4\pi \sin\theta}{\lambda}$. Here, the scattering vector is approximately parallel to the applied electric field direction.

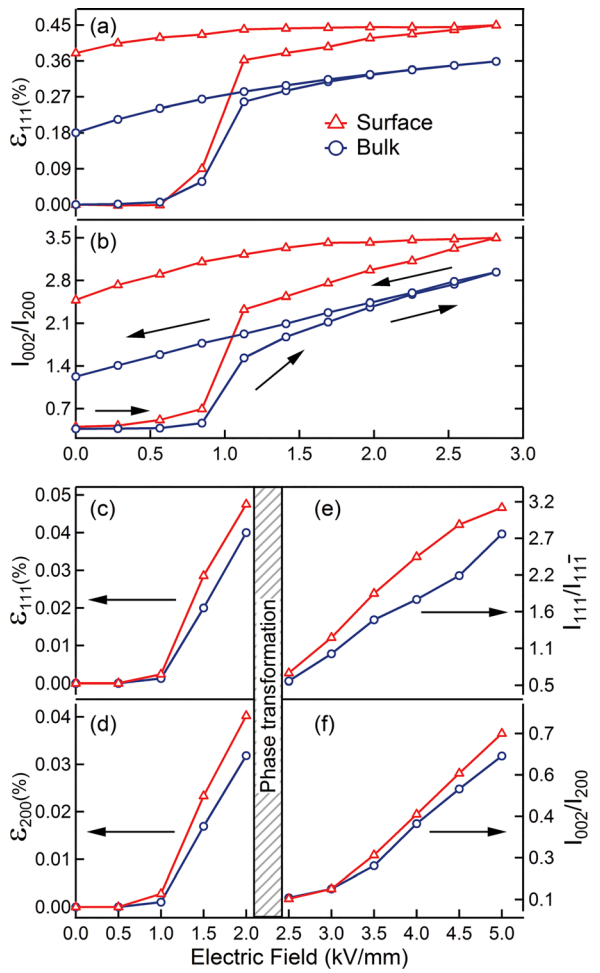

FIG. 3. (a) Lattice strain ε_{111} and (b) domain texture indicated by the intensity ratio of I_{002}/I_{200} for PZT, (c) ε_{111} and (d) ε_{200} for the pseudo-cubic phase of BNT-6.25BT before transformation, (e) $I_{111}/I_{11\bar{1}}$ and (f) I_{002}/I_{200} for the induced rhombohedral and tetragonal phases in BNT-6.25BT as a function of the applied electric field for the sample surface (red) and bulk (blue).

(I_{002}/I_{200}) are 20% and 16% higher at the surface than in the bulk, respectively. For BNT-6.25BT, at 2 kV/mm, the ε_{111} and ε_{200} are 15% and 20% higher at the surface than in the bulk. At 5 kV/mm, the domain textures in the mixed phase state, $I_{111}/I_{11\bar{1}}$ and I_{002}/I_{200}, are 12% and 10% higher at the surface than in the bulk.

In order to explain these results, the difference in the interactions between the probed grains of the two measurements is considered. At the surface, the grains are less constrained by their neighbor grains than the bulk grains. The surface sensitive measurement performed here weighs the scattering information from the top few grain layers above any information from deeper bulk grains. These grains are effectively more free to strain than those in the bulk, as the free surface is in a plane stress state. The lack of constraint means that grains in this close proximity to the surface can strain without a resistive force imposed by the surrounding material.

An additional result revealed from Figure 3 is that the magnitude of difference between the surface and bulk strain mechanisms is higher for the PZT than for BNT-6.25BT. In both cases, the applied maximum field strength is approximately three times the coercive field. To rationalize this difference, it must be recalled that the strain generation mechanisms in PZT and BNT-6.25BT are different. In PZT, the strain primarily originates from non-180° domain switching which gives rise to a ferroelastic strain and a crystal lattice distortion associated with the intrinsic piezoelectric effect and the compliance strain.[11,14] In the case of BNT-6.25BT, a crystallographic phase transformation to a mixed rhombohedral and tetragonal structure also contributes to the macroscopic strain in addition to these mechanisms.

The magnitude of intergranular stresses developed in polycrystalline piezoceramics experiencing a field-induced macroscopic strain is related to the degree of crystallographic anisotropy of the strain response. If only a single crystallographic axis experiences a large field-induced strain, large intergranular stresses are created in the polycrystalline structure where those "high response" grains are likely to be surrounded by many "low response" grains, whereas in materials which experience more isotropic field induced strain along multiple grain orientations, less intergranular stress is generated, as all grains in the system strain are approximately equal.

Therefore, the difference in the magnitude between the surface and bulk response of the two materials measured can be explained by the anisotropy of their response mechanisms. In the case of tetragonal PZT, grains that experience the highest strain are those preferentially aligned with the c-axis along the external field. These grains undergo large amounts of non-180° domain switching, generating a large ferroelastic strain for grains of this orientation, i.e., a ⟨001⟩ oriented parallel to the electric field. In the case of the BNT-6.25BT at 2.5 kV/mm, the pseudo-cubic phase has transformed into mixed rhombohedral and tetragonal phases. This phase transformation generates a transformation strain in both tetragonal ⟨001⟩ and rhombohedral ⟨111⟩ crystallographic directions; thus, the response is more isotropic. It is suggested that this isotropic response is the reason why the difference between the bulk and surface response in BNT-6.25BT is less than that for PZT. From the above discussion, it can be generalized that when a material response is more isotropic, the intergranular stress effect will be less pronounced, and thus, the bulk and surface response will be more similar. The lower intergranular stress, and the reduced variation in the behavior between the surface and bulk, will possibly lead to increased fracture toughness and improved fatigue lifetime.[30]

In summary, the electro-mechanical coupling mechanisms in the polycrystalline PZT and lead-free BNT-6.25BT have been measured using a surface sensitive low-energy and bulk sensitive high-energy synchrotron XRD. Higher magnitudes of both lattice strain and non-180° domain switching are observed at the surface compared with the bulk for both materials. It is suggested that the strain mechanisms can occur more easily at the surface than in the bulk because the grains at the surface are less constrained. The experimental results indicate that the difference in the electro-mechanical response from the sample surface and bulk is less when the strain mechanism is more isotropic. This is demonstrated by the larger difference between the surface and bulk response in PZT as opposed to the BNT-6.25BT material.

This project was supported by the Australian Research Council (ARC) through Discovery Project Nos. DP120103968 and DP130100415 and the Danish Independent Research Council|Technology and Production Sciences Case No. 12-127449. The authors acknowledge the provision of experimental beamtime by the Australian Synchrotron and the European Synchrotron Radiation Facility.

[1]J. Rödel, K. G. Webber, R. Dittmer, W. Jo, M. Kimura, and D. Damjanovic, J. Eur. Ceram. Soc. **35**, 1659 (2015).
[2]Y. Hiruma, H. Nagata, and T. Takenaka, J. Appl. Phys. **104**, 124106 (2008).
[3]T. Takenaka, K. Maruyama, and K. Sakata, Jpn. J. Appl. Phys., Part 1 **30**, 2236 (1991).
[4]L. Egerton and D. M. Dillon, J. Am. Ceram. Soc. **42**, 438 (1959).
[5]Y. Makiuchi, R. Aoyagi, Y. Hiruma, H. Nagata, and T. Takenaka, Jpn. J. Appl. Phys., Part 1 **44**, 4350 (2005).
[6]W. Jo and J. Rödel, Appl. Phys. Lett. **99**, 042901 (2011).
[7]S. T. Zhang, A. B. Kounga, E. Aulbach, H. Ehrenberg, and J. Rodel, Appl. Phys. Lett. **91**, 112906 (2007).
[8]V. D. Kugel and L. E. Cross, J. Appl. Phys. **84**, 2815 (1998).
[9]J. L. Jones, J. E. Daniels, A. J. Studer, and M. Hoffman, Appl. Phys. Lett. **89**, 092901 (2006).
[10]S. Trolier-McKinstry, N. B. Gharb, and D. Damjanovic, Appl. Phys. Lett. **88**, 202901 (2006).
[11]A. Pramanick, D. Damjanovic, J. E. Daniels, J. C. Nino, and J. L. Jones, J. Am. Ceram. Soc. **94**, 293 (2011).
[12]H. Simons, J. E. Daniels, J. Glaum, A. J. Studer, J. L. Jones, and M. Hoffman, Appl. Phys. Lett. **102**, 062902 (2013).
[13]M. Hinterstein, M. Hoelzel, J. Rouquette, J. Haines, J. Glaum, H. Kungl, and M. Hoffman, Acta Mater. **94**, 319 (2015).
[14]D. A. Hall, A. Steuwer, B. Cherdhirunkorn, T. Mori, and P. J. Withers, Acta Mater. **54**, 3075 (2006).
[15]J. E. Daniels, M. Majkut, Q. Cao, S. Schmidt, J. Wright, W. Jo, and J. Oddershede, Sci. Rep. **6**, 22820 (2016).
[16]B. Noheda, D. E. Cox, G. Shirane, S.-E. Park, L. E. Cross, and Z. Zhong, Phys. Rev. Lett. **86**, 3891 (2001).
[17]K. S. Wallwork, B. J. Kennedy, and D. Wang, AIP Conf. Proc. **879**, 879 (2007).
[18]B. Schmitt, Ch. Brönnimann, E. F. Eikenberry, F. Gozzo, C. Hörmann, R. Horisberger, and B. Patterson, Nucl. Instrum. Methods Phys. Res., A **501**, 267 (2003).
[19]M. J. Hossain, L. Wang, Z. Wang, N. H. Khansur, M. Hinterstein, J. A. Kimpton, and J. E. Daniels, J. Synchrotron Radiat. **23**, 694 (2016).

[20]J. Nuffer, D. C. Lupascu, and J. Rödel, Ferroelectrics **240**, 1293 (2000).
[21]J. E. Daniels, A. Pramanick, and J. L. Jones, IEEE Trans. Ultrason., Ferroelectr., Freq. Control **56**, 1539 (2009).
[22]J. E. Daniels and M. Drakopoulos, J. Synchrotron Radiat. **16**, 463 (2009).
[23]A. P. Hammersley, S. O. Svensson, M. Hanfland, A. N. Fitch, and D. Hausermann, Int. J. High Pressure Res. **14**, 235 (1996).
[24]J. E. Daniels, J. L. Jones, and T. R. Finlayson, J. Phys. D: Appl. Phys. **39**, 5294 (2006).
[25]A. Pramanick, J. E. Daniels, and J. L. Jones, J. Am. Ceram. Soc. **92**, 2300 (2009).
[26]A. Pramanick, A. D. Prewitt, M. A. Cottrell, W. Lee, A. J. Studer, K. An, C. R. Hubbard, and J. L. Jones, Appl. Phys. A **99**, 557 (2010).
[27]H. Simons, J. Daniels, W. Jo, R. Dittmer, A. Studer, M. Avdeev, J. Rödel, and M. Hoffman, Appl. Phys. Lett. **98**, 082901 (2011).
[28]M. Hinterstein, L. A. Schmitt, M. Hoelzel, W. Jo, J. Rödel, H. J. Kleebe, and M. Hoffman, Appl. Phys. Lett. **106**, 222904 (2015).
[29]W. Jo, J. E. Daniels, J. L. Jones, X. Tan, P. A. Thomas, D. Damjanovic, and J. Rödel, J. Appl. Phys. **109**, 014110 (2011).
[30]Y. A. Genenko, J. Glaum, M. J. Hoffmann, and K. Albe, Mater. Sci. Eng.: B **192**, 52 (2015).